bioRxiv submission draft v4, 19 Oct 2022

Canary in the cardiac-valve coal mine: Flow velocity and inferred shear during prosthetic valve closure –predictors of blood damage and clotting

Lawrence N. Scotten [1], Dipl. T., Rolland Siegel [2], BA, David J. Blundon [3], Ph.D., Marcus-André Deutsch [4], M.D., Terence R. P. Martin [5], D.Phil., James W. Dutton [6], M.D., Ebrahim M. Kolahdouz [7], Ph.D., Boyce E. Griffith, Ph.D. [8, 9, 10]

** In an early coal mining era, small songbirds accompanied workers in subterranean extraction sites. As these avian species are highly sensitive to changes in ambient air quality, they provided early warnings of impending hazardous breathing conditions.*

Affiliations:
[1] Independent consultant, Victoria, BC, Canada
[2] Independent consultant, Portland, Oregon, USA
[3] Instructor, Environmental Technology Program, Camosun College, Victoria, BC, Canada
[4] Surgeon – Cardiothoracic, Klinik fur Thorax- und Kardiovaskularchirurgie, Herz- und Diabeteszentrum NRW, Bad Oeynhausen, Germany
[5] Medical Engineer, Nottingham, UK.
[6] Cardiac Surgeon (retired) – Victoria, BC, Canada
[7] Center for Computational Biology, Flatiron Institute, Simons Foundation, New York, NY, USA
[8] Professor –Departments of Mathematics, Applied Physical Sciences, and Biomedical Engineering, University of North Carolina, Chapel Hill, NC, USA
[9] Carolina Center for Interdisciplinary Applied Mathematics, University of North Carolina, Chapel Hill, NC, USA
[10] Computational Medicine Program, University of North Carolina, Chapel Hill, NC, USA

Correspondence to: Lawrence N. Scotten. Dipl. T., Independent Consultant, Victoria, BC, V8P 4V4, Canada.
Email: larryscotten2@hotmail.com

*See Appendix 2, F.

Graphical Abstract

Static flow tests illustrate free jets of water passing through a closed mechanical valve (SJM). Investigations with pulsatile flow suggest similar fleeting jets arise near valve closure. Flow velocity determined in-vitro is evidence for shear forces that are predictive of blood cell damage and thrombogenic response. Red star is moment of valve closure.

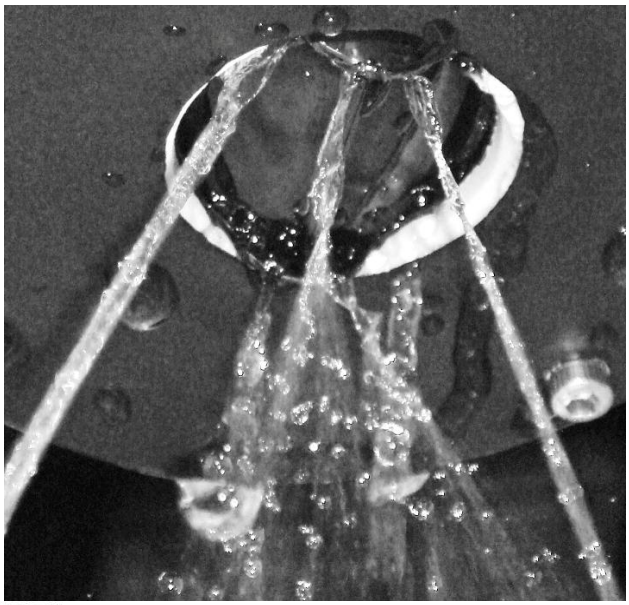

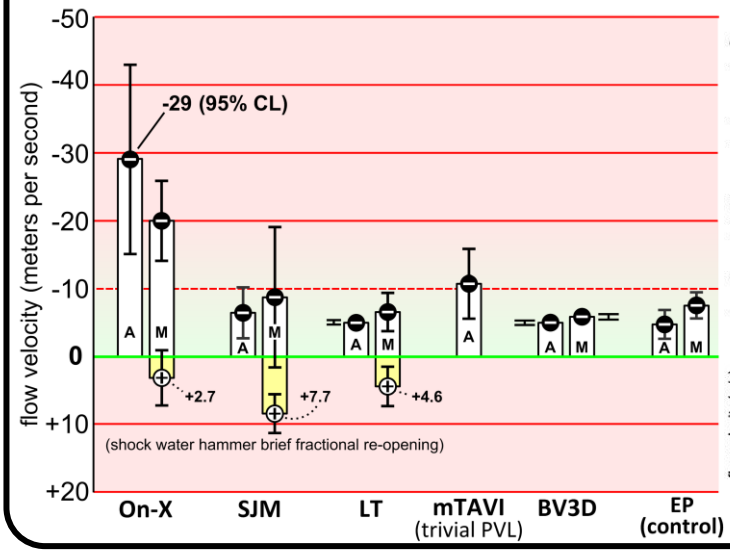

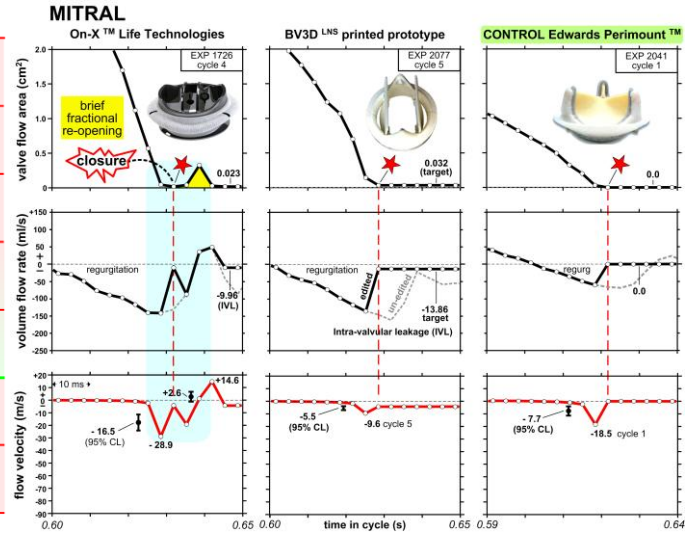

ABSTRACT

Objective: To demonstrate a clear link between predicted blood shear forces during valve closure and thrombogenicity that explains the thrombogenic difference between tissue and mechanical valves and provides a practical metric to develop and refine prosthetic valve designs for reduced thrombogenicity.

Methods: Pulsatile and quasi-steady flow systems were used for testing. The valve flow area time-course was measured using analog opto-electronics calibrated to the projected dynamic valve area. Flow velocity determined over the cardiac cycle equates as instantaneous volumetric flow rate divided by valve flow area. For the closed valve interval, data obtained from quasi-steady back pressure/flow tests was used. Performance ranked by derived maximum negative and positive closing flow velocities, evidences potential clinical thrombogenicity via inferred velocity gradients (shear). Clinical, prototype and control valves were tested.

Results: Blood shear and clot potential from multiple test datasets guided empirical optimization and comparison of valve designs. A 3-D printed valve (BV3D) design emphasizes soft closure for reduced thrombogenic potential.

Conclusions: The relationship between leaflet geometry, flow velocity and predicted shear at valve closure illuminated an important source of prosthetic valve thrombogenicity. With an appreciation for this relationship and based on our experiment generated comparative data, we achieved optimization of valve prototypes with potential for reduced thrombogenicity.

Competing Interests: None declared.
Financial Disclosure: This research has been done on a pro bono basis by all authors.

Key Words: prosthetic valve; laboratory simulation; valve area; valve closure, thrombogenicity; valve flow velocity; rebound

CENTRAL MESSAGE

A derived laboratory metric for valve closing flow velocity offers a way to rank valve models for potential blood damage. These results provide new insight and a mechanistic explanation for prior clinical observations where aortic and mitral valve replacements differ in thrombogenic potential and anticoagulation requirement. The study suggests a path forward to design and evaluate novel mechanical valve models for future development. As multiple modifications to mechanical and bioprosthetic valves have not resolved chronic shortcomings related to thrombogenicity and durability, a new development avenue was required in order to eliminate thrombogenicity in the former and extend durability in the latter.

PERSPECTIVE

Prosthetic mechanical valve devices cause blood cell damage. Activation of the coagulation cascade is initiated by dynamic valve function. Design innovation focusing on valve closure behavior may reduce valve thrombogenic potential. **Our study demonstrates that valve design can be optimized with emphasis on that phase.**

SIGNIFICANCE

Attribution of valve leaflet geometry to occluder dynamic behavior and derived regional flow velocity may lead to the development of less thrombogenic valve replacements. Laboratory experiments support the supposition that valve regional flow velocity is associated with valve thrombogenic potential. This study compares three clinical valves and two experimental prototypes.

INTRODUCTION AND BACKGROUND

Our interest in prosthetic valve dynamics was initially stimulated during formation of the Cardiac Research Development Laboratory tasked with supporting the newly opened Cardiac Surgery unit at Royal Jubilee Hospital in Victoria, BC, Canada (1973). Incorporated as Vivitro Systems Inc (VSI), our primary focus was research, design and development of cardiac valve implant devices and on the laboratory test systems required. During this phase we studied valve motion in an early pulse duplicator using high-speed cinematography and photogrammetric analysis [1, 2]. Subsequently, an innovative simpler method was devised to determine dynamic prosthetic valve area similar to planimetric quantification and was published in *New Laboratory Technique Measures Projected Dynamic Area of Prosthetic Heart Valves* [3]. In 2009, work transitioned into a separate independent research and development enterprise, ViVitro Laboratories Inc. (VLI) also based in Victoria, BC, Canada.

Consistent with a focus on evaluation of various prosthetic valve models, our pulse duplicator was modified to include a unique opto-electronic subsystem which we named *Leonardo*. The addition of this subsystem redirected our interest in heart valve dynamics to the closure phase and associated supra-physiologic backflow fluid velocities. Driven by ongoing curiosity and armed with new data from *Leonardo*, we reported our findings through a series of preprints and publications [4-12]. In a recent broader application of our investigative technology, results from *in silico* computational modeling and *in vitro* experimental studies provided validation of the characteristics of bioprosthetic valve leaflet flutter along with invited peer commentary [11-15].

Given the arc of success with prosthetic valves over decades including initiation and progressive expansion of transcatheter devices, long-term durability and thrombosis issues persist. Thrombosis is a physics-based phenomenon that nature evolved to stem bleeding after an injury. For both transcatheter and surgically implanted bioprosthetic valves, limited durability related to multiple factors has stimulated introduction of a variety of “rescue devices”. Intended to provide transcatheter based mitigation of complications in primary and valve-in-valve bioprosthetic valves implants, these devices are associated with their own unique complications.

The longer term consequences of a transcatheter based multiple valve approach for patient morbidity, mortality and overall cost are yet to be determined. In the current paper, our focus returns to identification and assessment

of sources of thrombogenicity in contemporary clinical and also experimental mechanical and bioprosthetic heart valves with particular attention to the central role of conspicuous transient fluid velocities during valve closure. Flow velocity manifests shear via flow velocity gradients that trigger blood damage and clot formation in vascular disease processes and cardiovascular implant devices [16, 17]. Evidence comparing dynamic behavior across a range of both clinical and experimental devices then stimulated provocative conclusions regarding development of less thrombogenic yet durable prosthetic valves.

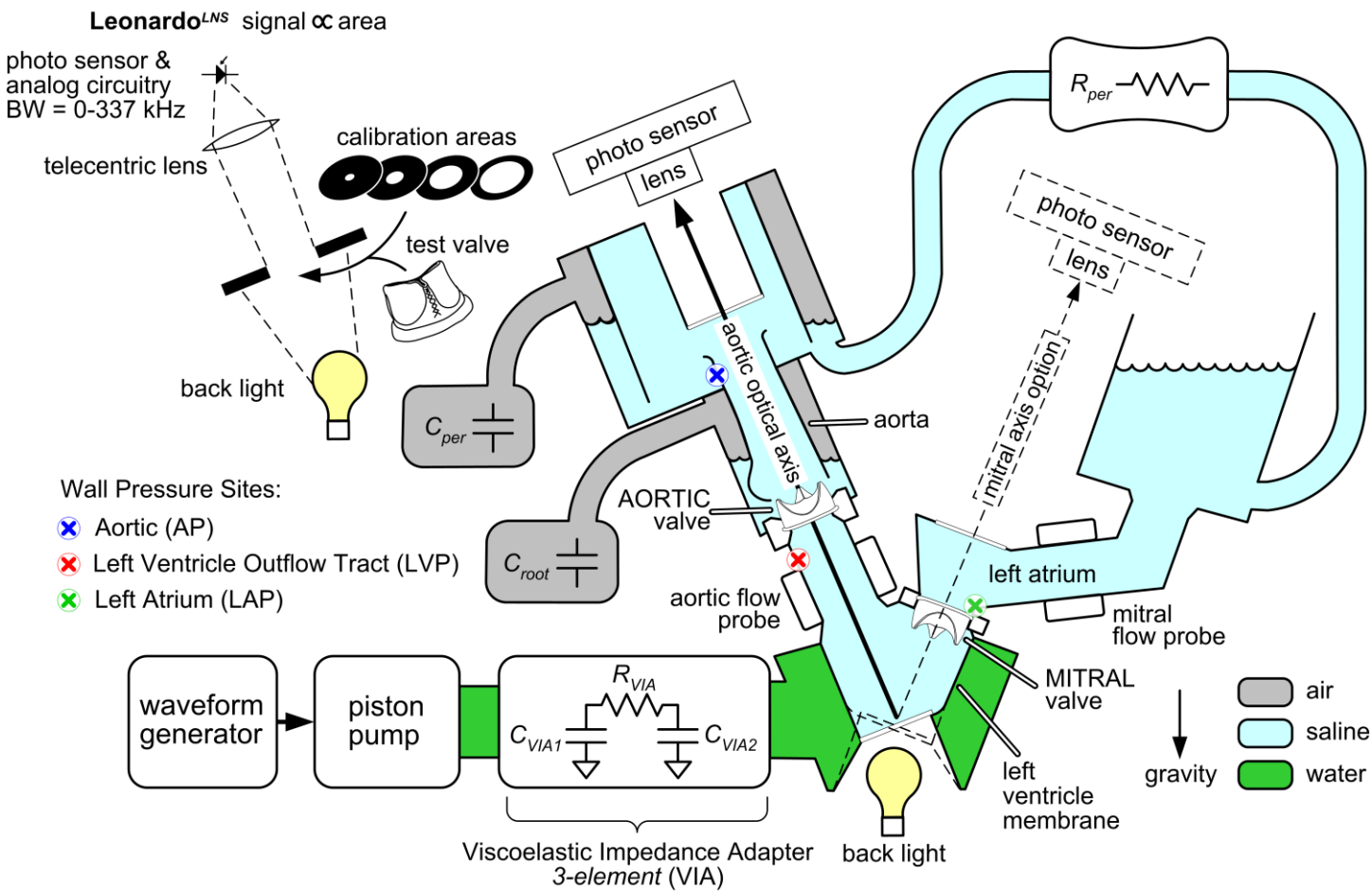

FIGURE 1. Schematic of modified pulse duplicator utilized for testing of prosthetic heart valves in vitro.

<u>Pulse Duplicator Test Conditions and ~Settings:</u>
–upstream: C_{VIA1} 120 mL; C_{VIA2} 50 mL; R_{VIA} 200 c.g.s. units
–downstream: C_{root} 640 mL; C_{per} 615 mL;
test valve sizes 25 mm; test fluid saline; cardiac output 5 l/min
R_{per} adjustable and normally tuned for mean aortic pressure 100 mmHg

METHODS

Pulse Duplicator Experiments and Computational Modeling

Over time, progressive adaptations to the pulse duplicator apparatus have been reported [1-12]. This included the optical measurement of valve kinematics and *in silico* evaluations [3-15]. Aforementioned conditions and settings used in this study are applicable to Figure 1 and are related to fluid-structure interaction (FSI) studies and associated boundary conditions [11-15]. Also, in comparing results from a computational model with results from the pulse duplicator, experimental outcomes showed close agreement [11, 12, 14, 15]. Test valves are listed in Table 1. Flow and pressure signals are filtered by analogue circuitry (bandwidth BW~ 0-100 Hz). The valve flow area signal was unfiltered and had a measured rise time ~ 1.04 μs (BW ~ 0-337 KHz). Saline

was used as an accepted test fluid per ISO 5840-3 with density $\rho = 1.0$ g/cm^3 and dynamic viscosity $\mu = 1.0$ cP [18].

TABLE 1. Valves tested in aortic and mitral locations

Valve Name	Description	Site
St. Jude Medical Regent ™ (SJM)	Mechanical bi-leaflet	**A, M**
mock-TAVI (PVL pre-adjusted)	Prototype mounted with preset trivial paravalvular leak (PVL)	**A**
On-X ™ Life Technologies	Mechanical bi-leaflet	**A, M**
BV3D LNS	Printed prototype, bi-leaflet	**A, M**
Lapeyre-Triflo ™ -F6	Prototype, mechanical tri-leaflet	**A, M**
Edwards Perimount ™	Bioprosthetic, pericardial tri-leaflet	**A, M**

All test valves tissue annulus diameter (TAD) ~ 25 mm. (**A**)ortic, (**M**)itral; Non-test valve -Mitroflow** pericardial size 29 mm. **Sorin, Milan, Italy

Pressure measurement

Left atrial, left ventricle aortic outflow tract, and aortic sites pressures were measured via short catheters (~ 7.5 cm length) with internal diameter of ~1.8 mm connected to disposable pressure transducers (Deltran™, model PT43-604)***. Catheter ports were located at sites where measured pressure was referenced to the mid-plane of the tested valve. In Figure 1, aortic transvalve pressure is measured between the left ventricular outflow tract (LVP) and the aorta (AP). Mitral transvalve pressure is measured between the left atrium (LAP) and the left ventricular outflow tract (LVP).

Significant waveform characteristics

Several traits are clear in Figures 3-5. All signals were sampled synchronously. Regions relevant to the valve closure moment are near the dashed red line. Of importance are: initial minimum valve flow area values (VFA) and initial peak negative values attained in transvalve pressure, volume flow rate, and closure flow velocities. For bioprosthetic valves, we observed an upward-downward movement of both the valve frame and leaflets demonstrative of compliance reactivity. Hydrodynamic oscillations are also present post valve closure as seen in the unadjusted volume flow rate in some of the waveforms. Comparing the phasing of volume flow rate and valve flow area near valve closure, regional components having compliance influenced hydrodynamic patterns.

Signal synchronicity

As indicated in Figures 3 and 4, in the aortic and mitral valve sites, instantaneous minimum regurgitant volume flow rate and minimum valve flow area are synchronous with valve closure. Results for aortic and mitral valves show that maximum negative instantaneous volume flow rates (regurgitation) are synchronous with valve closure. The flow and pressure signals are processed through 100 Hz low-pass analogue filters whereas the valve area signal is unfiltered which preserves maximum frequency response (~ 0-337 KHz).

Synchronized hydrodynamic oscillations emerge post valve closure due to the pooled reactive compliances of the test valve and holder. These damped oscillations are observed in the unadjusted volume flow rate signals (dashed grey) ascribed to the combined movement of test valve components (i.e., leaflets plus stent) within the elastic silicone rubber holder. Oscillations evident for all valves and sites have similar periodicity ~ 20ms (50 Hz).

Statistical Analysis

For each experiment, we acquired 10 consecutive cycles and report the mean and confidence limits (CL) of the 10 negative peak flow velocities recorded. Summary of the valve flow velocity test datasets utilize EXCEL**** data analysis tool labeled descriptive statistics with options -Analysis ToolPak and -Solver Add-in. In Figure 3-5, mean negative peak flow velocities and CL=95% indicated by verti-bars (whiskers) adjacent to the flow

******* Utah Medical Products Inc., Midvale, Utah 84047-1048, USA ******** Microsoft, Redmond, WA, USA

A
printed prototype

B
rendering

FIGURE 2. (A) photograph (B) rendering of prototype bi-leaflet mechanical valve BV3D see video https://youtu.be/5QmDPbfUvTM animation link

velocity waveforms show the predicted uncertainty.

Experimental valve design

The BV3D rapid prototype valve design shown in Figures 2A and 2B show a working model that resulted from several designs trialed [7]. Consideration of competing factors produced 56 laboratory constructed prototype valves with empiric data from experiments producing optimization through interaction of leaflet profile, pivot location and surface characteristics. These led to the rapid printed prototype model BV3D with advantageous forward and especially closing flow dynamics. In this work, *Leonardo* provided immediate feedback on the impact of even subtle geometric changes on valve dynamic behavior.

RESULTS

Aortic *vs.* Mitral Dynamics

When fluid in motion is abruptly halted or changes its direction (momentum change) water hammer is observed. This unwanted transient motion closely associates with valve closure timing, property of valve mountings and has been previously reported in vitro [5]. Figure 3-5 illustrate shock water-hammer dynamics with mean flow velocities reaching -29.0 m/s for the On-X mitral and -65.2 m/s for the On-X aortic valve and is absent for the Lapeyre-Triflo -F6, prototype BV3D, mock-TAVI, and Edwards-Perimount control valves. The mock-TAVI valve was untested in the mitral site.

For the On-X, SJM, and LT valves in the mitral site, a brief fractional reopening is evident in valve flow area post initial closure. In Figure 4, negative peak transvalve pressure spikes range over comparable levels in the mitral site (-75 to -90 mmHg). However, in the aortic position (Figure 3) pressure spikes encompass a wider range (-40 to -95 mmHg).

Signature shock water hammer dynamics for aortic and mitral valves are evident for valve flow area, transvalve pressures, volume flow rates, and derived valve flow velocity waveforms. We found that shock water hammer

dynamics can be mitigated by valve designs optimized for soft valve closure which reduces retrograde valve flow velocity in the early closing phase as observed for the BV3D and EP valves.

Edited *vs.* unedited instantaneous flow rates

In Figures 3 and 4, measured and derived aortic and mitral valve test results include 10 consecutive cycles each experiment. Data acquisition sampling interval is ~3.36 ms (white data points). Evident are maximum negative valve closure flow velocities ranging up to -65.2 m/s (On-X aortic). The oscillatory character seen in the primary unadjusted (grey) flow rate waveforms were edited to produce the black volume flow rate waveform data prior to deriving the flow velocity data (red waveforms). The spatially averaged metric of mitral flow velocities (red curves) are obtained by dividing time-periodic volume flow rate by time-periodic valve flow area. Average flow velocity and confidence limits are depicted by whiskers and show where 95% of the derived negative peak valve flow velocities fall. An inherent advantage of the *Leonardo* sub-system is that flow area is determined by a high resolution optical approach projecting geometric valve boundaries. In Figure 4, the mock-TAVI valve produced aortic but not mitral site data. Leakage rates are indicated either intra-valvular (IVL) or paravalvular (PVL). Post valve closure, valve fractional re-openings, highlighted in yellow, are attributable to shock water hammer phenomena.

Readers will note that in prior publications, closing flow velocities in excess of those observed in this study were reported [5-10]. *Previous records with excessive closing flow velocities have been rectified in this report by re-analysis of the historical experiment test datasets imported into revised EXCEL templates.*

Other noteworthy points in Figures 3-5 are:

- For the SJM valve, the differential between aortic and mitral maximum volumetric backflow rates consistently exceeded that observed in other tested valves ~ (-180 ml/s$_{-max}$ *vs.* -150 ml/s$_{-max}$).
- For current clinical mechanical mitral valves, abrupt closure and ensuing shock water hammer dynamics highlighted in yellow, triggers a brief partial valve re-opening ~ 6 ms after valve closure and rebound duration of ~ 4-10 ms.
- Mitral valve closure generates flow rate and transvalve pressure oscillations of greater amplitude but less dampened than valves in the aortic site.
- In the mitral site, valve occluder rebound (highlighted yellow) associates with high negative regurgitant volume flow rate and transvalve pressure peaks and flow velocities impacting on valve re-closure.
- Transvalve negative pressure spikes are nearly synchronous with valve closure.
- Important features underscored in the valve closure phase are: near synchronous timing of valve closure (i.e., valve minimum flow area), negative transvalve closure pressure spikes, maximum retrograde closure volume flow rate, and maximum retrograde flow velocities.
- The velocity of unsteady pressures in water is ~1,500 m/s. Therefore, pressures in immediate proximity to the aortic test valve for example would have trivial phase (~0.07 ms) relative to the aortic wall pressure site which is ~10 cm distant from the mid-plane of the valve.

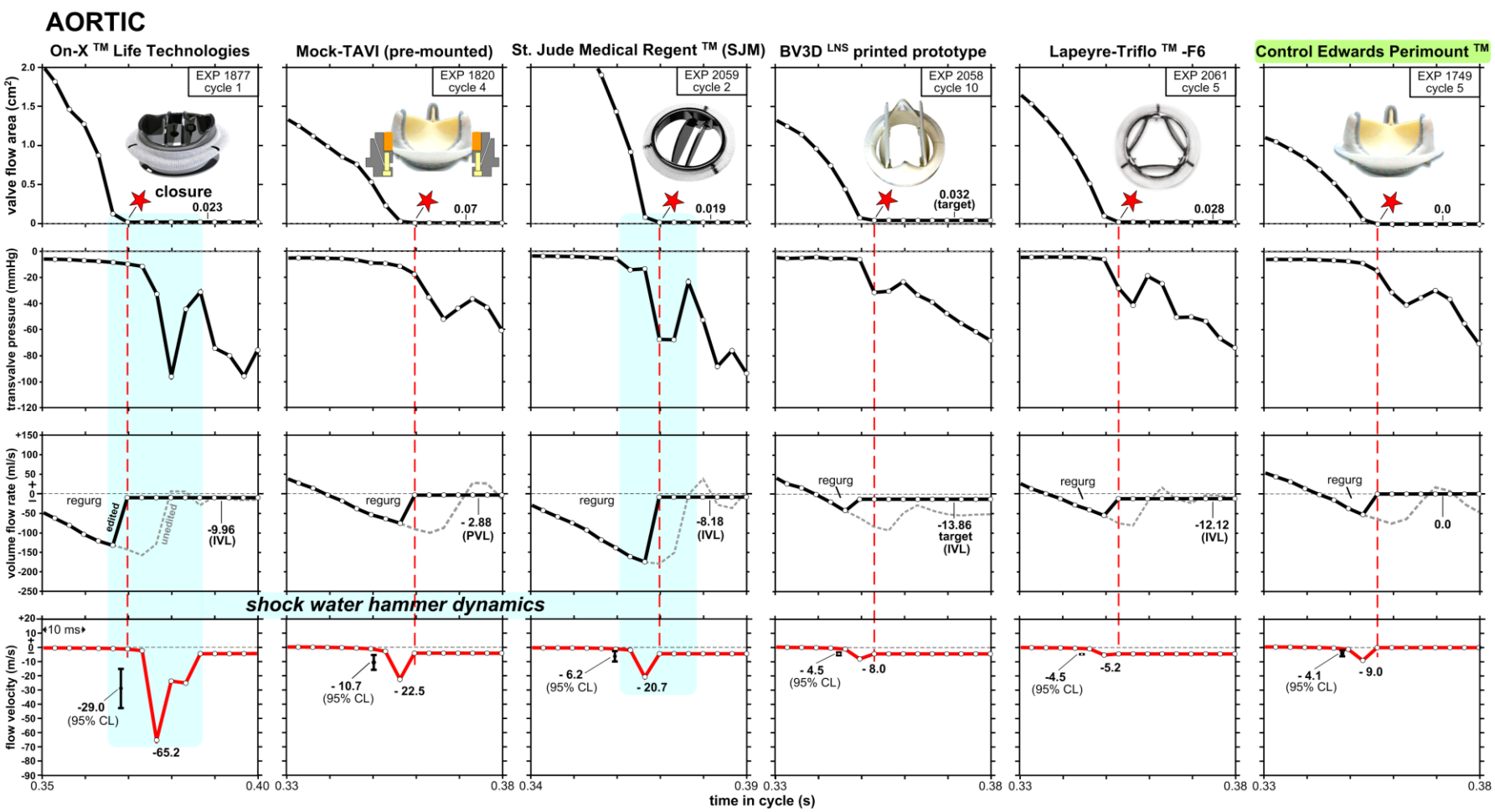

FIGURE 3. Measured and derived AORTIC valve test data includes 10 consecutive cycles each experiment. A spatially averaged metric for aortic valve flow velocity (red curves) equals volume flow rate / valve geometric flow area. Average flow velocity and confidence limits (CL) depicted by black verti-bars (whiskers) show where 95% of the derived negative peak flow velocities fall. Maximum and mean negative flow velocities are shown. An optical approach measures dynamic valve flow area from the projected geometric boundaries of valve function obtained in vitro. Data acquisition sampling interval shown by white data points is 3.36 ms. Intravalvular leakage rates are shown (IVL) and paravalvular (PVL). Edited *vs.* unedited volume flow rate waveforms are dashed grey alongside solid black edited flows. Unedited flows (dashed grey) show influence of reactive elastic and inertia elements which are edited out prior to final flow velocity estimation. Shock water hammer zones are highlighted in blue. Control valve is Edwards Perimount.

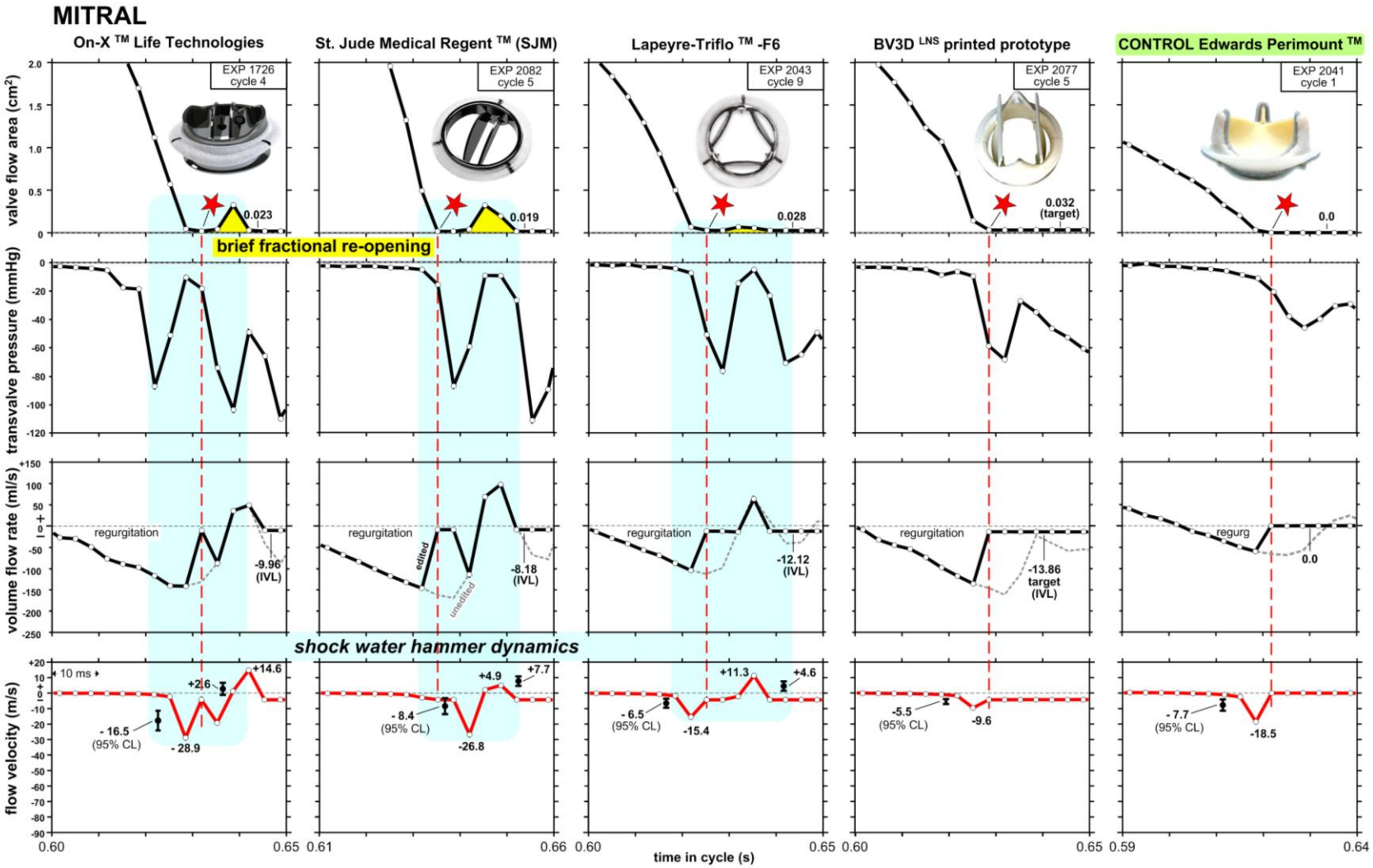

FIGURE 4. Measured and derived MITRAL valve test data includes 10 consecutive cycles each experiment. A spatially averaged metric for mitral valve flow velocity (red curves) equals volume flow rate / valve geometric flow area. Average flow velocity and confidence limits (CL) depicted by black verti-bars (whiskers) show where 95% of the derived negative and positive peak flow velocities fall. Maximum and mean negative flow velocities are shown. An optical approach measures dynamic valve flow area from the projected geometric boundaries of valve function obtained in vitro. Data acquisition sampling interval shown by white data points is 3.36 ms. Intravalvular leakage rates are shown (IVL) and paravalvular (PVL). Edited *vs.* unedited volume flow rate waveforms are dashed grey alongside solid black edited flows. Unedited flows (dashed grey) show influence of reactive elastic and inertia elements which are edited out prior to final flow velocity estimation. Partial re-opening of MITRAL valve areas are shown highlighted in yellow and the shock water hammer zones are in blue. Control valve is Edwards Perimount.

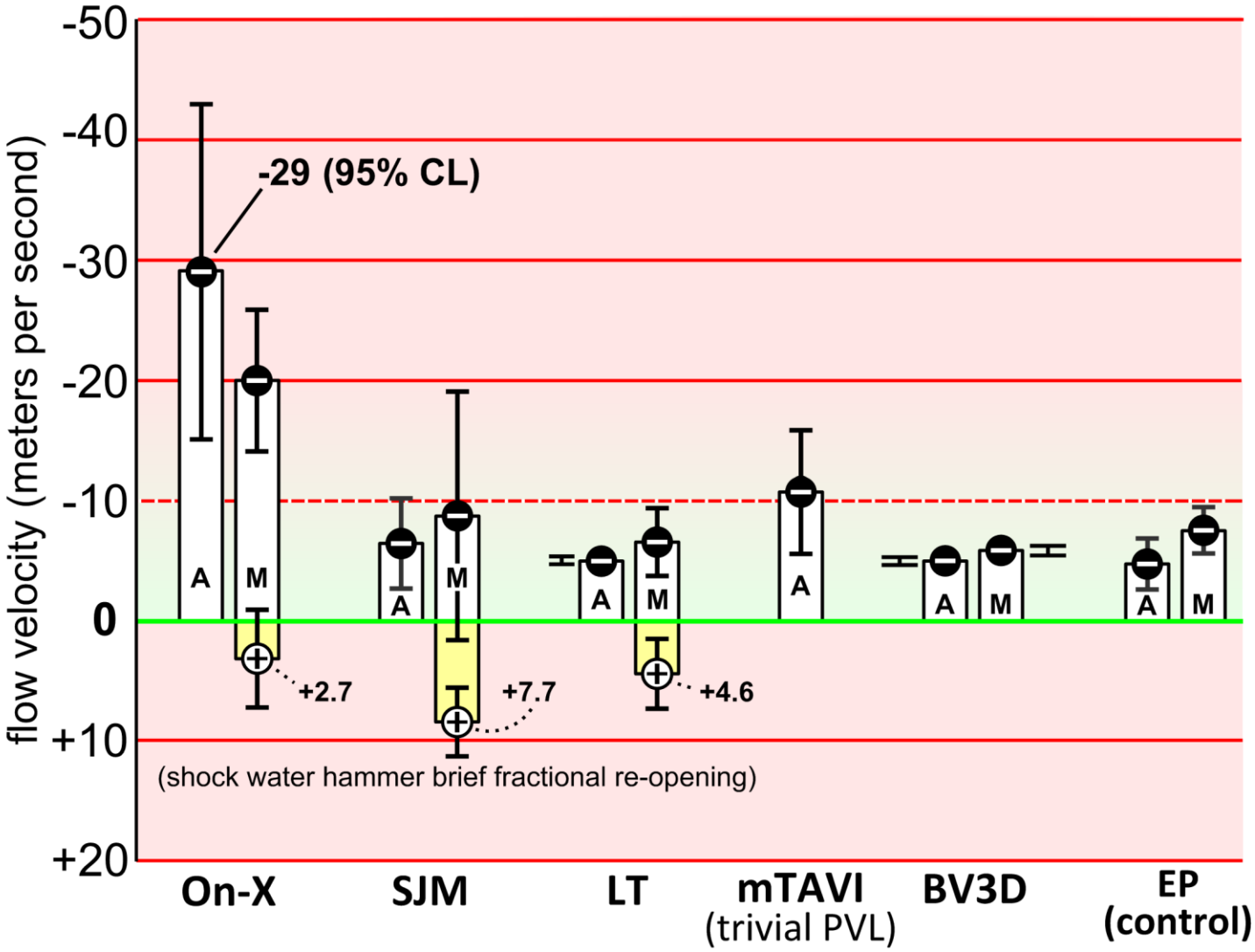

FIGURE 5A. For each valve and site (**A**ortic, **M**itral), the average valve closing flow velocity of ten consecutive cycles and confidence limits show where 95% of the derived positive and negative flow velocities fall. Valves: -Mechanical (bi-leaflet: **On-X**, **SJM**, printed prototype **BV3D**), (tri-leaflet **LT** -F6), -Tissue (mock-TAVI, **mTAVI**, Edwards Perimount™ **EP**).

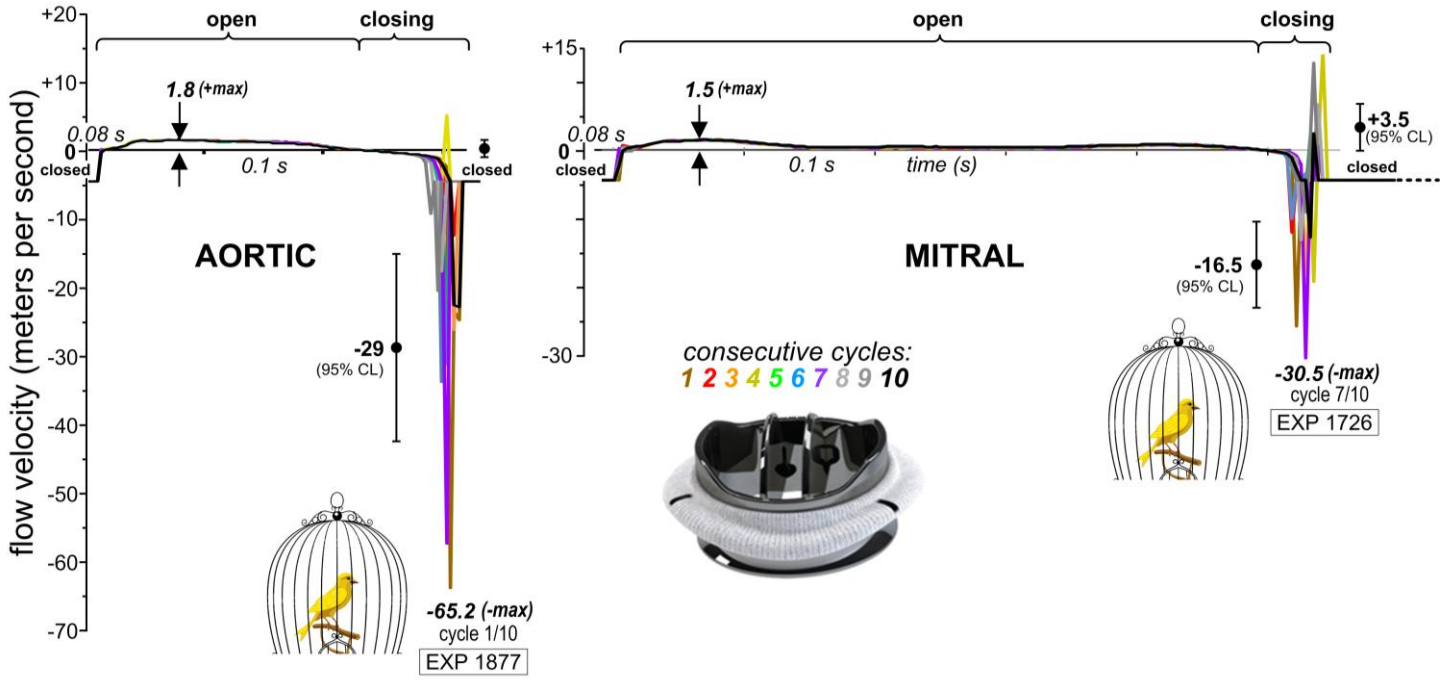

Figure 5B. For the On-X valve in aortic and mitral test locations, color-coded instantaneous flow velocities are shown for 10-consecutive cycles. Confidence limits (95%) are shown for the positive and negative flow velocities. Note maximum flow velocities of closing and opening aortic valve can diverge by 36× (65.2/1.8). Similarly, the closing mitral valve can diverge by 20.3×. Crucially, flow velocity for a closing valve is much greater than in the open state. Our multiple test datasets challenge the chronic emphasis (bias) associated with open valve performance as primary to valve thrombogenic complications while under emphasis of the closing phase has consistently overlooked the canary in the cardiac valve coal mine.

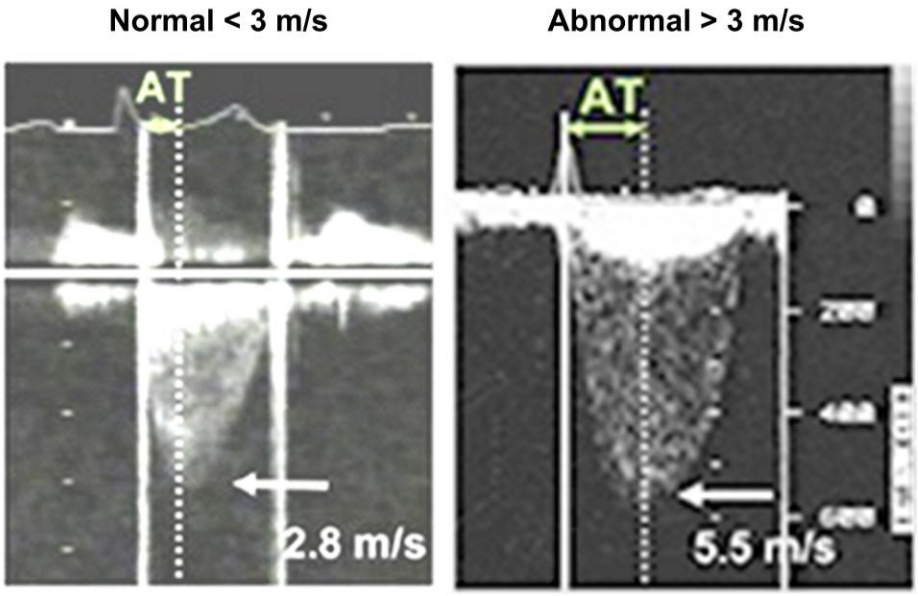

Figure 5C. Peak CW Doppler signals shown in Link are examples of normal and abnormal prosthetic valve flow velocities. Peak open flow velocities for the On-X valve shown in Figure 5B are thus considered normal.

Result overviews in Figure 5 A and B are based on predicted valve flow velocities. Notable are positive flow velocities for SJM, On-X and LT. An interesting mitral site pattern is that shock water hammer phenomena are associated with three of the four mechanical mitral valves tested (On-X, SJM, LT), a response evidencing momentary post closure fractional reopening and absence in the two bioprostheses (mTAVI and EP). The EP aortic and mitral control valves have low closure flow velocity (< 10 m/s).
Important elements in Figure 3-5A and B:

1. The EP aortic and mitral control valve demonstrated the lowest predicted valve closing flow velocity which is consistent with their reported clinical experience of low thrombogenic potential.
2. Driven by shock water hammer dynamics, backflow velocity is higher in the mitral than aortic site.
3. Slow-motion and real time visualization of aortic and mitral valves revealed qualitatively both symmetrical and non-symmetrical closing behavior of occluders. Quantitatively, flow velocity whisker length may be useful as a measure of occluder motion evenness over 10 consecutives cycles. Results show that the On-X and SJM have greatest whisker lengths.
4. The mTAVI valve sample with trivial paravalvular leak (PVL) had a peak average negative valve closing flow velocity of -10.7 m/s (±5.25). However, it has been noted that valve samples with PVL = zero and counter intuitively, with > PVLs, have reduced valve closing flow velocities [5, 6].
5. Based on the control valve results, mean closure flow velocities < -10 m/s suggests low/non-thrombogenic shear force potential.
6. Valve closing dynamics are associated with shock water hammer are also associated with maximums in flow velocity, backflow rate and transvalve pressure.

DISCUSSION

Over the past 60 years, heart valve design and performance evolved to provide improved durability and hemodynamic function. While preferences for mechanical *vs.* bioprosthetic valves fluctuated widely, the advent of transcatheter delivered devices and their less invasive insertion methodology, the balance shifted progressively in favor of bioprostheses. Although initially restricted to use in the elderly or patients designated too fragile for conventional surgical implantation, use is now extended to younger and lower risk candidates. This despite prior clinical data that demonstrated reduced durability of bioprosthetic valves in younger recipients. To respond to an incidence of technical failure in contemporary transcatheter valves and perhaps in anticipation of increasing frequency of degenerated valves in younger patients, a variety of transcatheter "rescue" devices are offered. Inserted within a degenerated or malfunctioning primary valve or a previously implanted rescue device, the predicted durability of rescue devices is speculative. In a prophetic article *Russian Dolls; when valve-in-valve implantation is not enough* [19], Tseng called attention to the possibility of rescue valve recipients who will represent therapeutic challenges that may not be resolvable by transcatheter devices. As a response to a possible increase in this initially small subset of patients, for those valve replacement candidates who favor the alternative of one valve durable for life but are hesitant because of concerns over anticoagulant related issues and the as-yet unfulfilled need by rheumatic patients in developing countries [20-23] it is essential that research driven by purposeful curiosity continues toward achievement of a long awaited anticoagulant independent mechanical valve by research endeavors such as recently reported by Wium et al. [22, 23].

At or near valve closure, flow dynamics can be considered analogous to transitory valve stenosis, whereby regurgitation is increasingly constrained until complete, motionless, closed-valve conditions arise. Thus, during brief crucial moments preceding valve closure, localized prothrombotic microenvironments may be relevant to generation of high velocity leakage jets that may induce blood element damage [24-26]. These influences may impact multiple valve types and potential consequences of these phenomena may include but not limited to:

- reduced valve leaflet mobility, sub-clinical thrombosis [27],
- potential for pannus formation,
- transient ischemic attack (TIA), embolic acute/sub-acute stroke, other silent micro-infarction and adverse cerebrovascular events [28],
- cavitation and high intensity transient signals (HITS) [30].

Shock water hammer phenomena and occluder rebound

Mitral valve closure dynamics shown in Figure 4 include a partial post closure transient opening (rebound) attributable to shock water hammer, were found less prominent in the aortic site (Figure 3). Occluder rebound driven by water-hammer power (product of transvalve pressure and volumetric flow rate) for the SJM mitral valve is observed as a momentary post closure partial re-opening. This has been previously reported with high resolution magnified examples of valve flow area rebound data [3, 5, 7]. Relative to the bioprosthetic control valve, mechanical mitral valves (On-X, SJM, LT) are driven by higher-level transvalve pressures and retrograde flows and reveal rebound behavior prior to final closure. Additional pro-thrombotic aspects may be related to sub-optimal valve forward flow energy losses (e.g. arterial sclerosis) and biomechanical and biochemical responses sufficient to exacerbate risk of pathologic thrombus formation and propagation.

Study outcomes (previous and present reports) [3-10]:

1. High amplitude valve closing flow velocities may result in supra-physiologic shear forces originating in small intra- and para-valvular leak gaps and which become mechanistic initiators of the clotting cascade.
2. Platelet activation is induced by high shear even with short exposure time (transient) [26].
3. Closing dynamics disparity between mechanical (MHV) and bioprosthetic valves is chronically overlooked as a primary indicator of valve thrombogenicity.
4. Current MHVs have overt valve closing flow velocity transients relating to occluder non-response to flow deceleration and residual valve flow area.
5. For a given volumetric backflow rate near valve closure, the smaller the total residual leakage area, the greater the valve closing flow velocity.
6. The highest valve closing flow velocity was for the SJM Aortic valve compared to the tissue control valve (Edwards pericardial).
7. The prototype BV3D valve had lowest predicted valve closing flow velocities in both aortic and mitral sites. Assessment of this dynamic behavior represents a practical means to qualitatively screen valves and controls for thrombogenic potential.
8. Valve BV3D test data suggest that specific MHV leaflet geometries generate a closing force during forward flow deceleration and prior to flow reversal, a potentially beneficial “soft closure” response.
9. Our results infer shear damage of formed blood elements and potential for continuing thrombogenic response. This constitutes a mechanistic explanation for observed thrombogenic disparity in prosthetic valve types and designs, now broadened to include observations of TAVR related thromboembolic events.
10. For MHVs, cyclic valve closing flow velocities appear to be related to a prothrombotic state requiring chronic anti-coagulation.
11. Bioprosthetic valves appear not to generate a pro-thrombotic closing phase.
12. In both experimental and computational pulse duplicator studies, bioprosthetic valves in smaller diameters and/or with thicker leaflets generate higher flutter frequencies [11, 12].

Limitations

We give consideration here to a derived valve closing flow velocity metric. Also, we noted a brief positive flow transient for some mechanical mitral valves. Such transients manifest along with a shock water hammer which

are indicative of high shear force, blood cell damage, biomechanical and biochemical responses that promote pathologic thrombus formation and propagation.

Strengths

Mechanical valve tested in the mitral position consistently manifested leaflet rebound observed as a transitory post closure partial re-opening driven by water-hammer power (product of transvalve pressure and volumetric flow rate). This has been previously reported with magnified examples of high resolution valve flow area rebound data [5].

High fidelity computational simulations are required to resolve small scale valve geometries and flows etc. This prerequisite may benefit from recently developed computational approaches and needed extensions to help fill lingering computational gaps [33, 34].

CONCLUSIONS

This work exposes the central relationship between thrombogenicity and predicted high velocity flows and shear forces at valve closure. As practical application of our findings, specific valve geometric features were identified that led to prototype designs with potential for further development. The application of unique technology, rapid prototyping and ranking of flow velocity patterns near valve closure optimized experimental valve geometry for reduced thrombus potential compared with control valves.

Our results identify and quantify crucial valve closure factors such as closing flow velocity but also raise a challenging question: does optimum mechanical valve performance mandate similar, identical or lower valve closing flow velocities to those of contemporary clinical bioprostheses?

Finally, as demonstrated in Figure 5b, valve flow velocity differentials and associated shear are significant activators of the thrombogenic canary. Accordingly, future valve designers are strongly encouraged to give appropriate emphasis to this crucial valve closure behavior.

While development and introduction of any new and innovative prosthetic heart valve is a lengthy, complex, and costly process, our work purpose opens an experimentally assisted pathway for development of durable but less thrombogenic devices. Prototype model BV3D is tangible evidence that focused laboratory efforts can yield rewarding breakthrough results. The holy grail of a mechanical valve independent of chronic anticoagulation still beckons.

Conflict of Interest Statement

All authors report no conflicts of interest.

Contributions:

(I) Methodology, conception and design: LN Scotten; (II) Project administrative support: LN Scotten; (III) Provision of study materials: LN Scotten; (IV) Collection and assembly of data: LN Scotten; (V) Data analysis, interpretation, validation: LN Scotten, DJ Blundon…; (VI) All authors have contributed.

Acknowledgements:

Competing Interests: None declared.

Financial Disclosure: This research has been done on a pro bono basis by all authors with no financial support of others.

Data availability statement: Core data that support the findings of this study are available from the corresponding author, [LNS], upon reasonable request.
Open access: Anyone can share, reuse, remix, or adapt this material, providing this is not done for commercial purposes and the original authors are credited and cited.

References

1. Brownlee RT, Scotten L. The in vitro assessment of left ventricular flow patterns on the closure of a new mitral valve "Bioprosthesis". Trans ASAIO 1976;22:341-346. Pub Med

2. Scotten LN, Walker DK, Brownlee RT. Construction and evaluation of a hydromechanical simulation facility for the assessment of mitral valve prostheses. J Med Eng Technol 1979;3:11-18. Pub Med

3. Scotten LN, Walker DK. New Laboratory Technique Measures Projected Dynamic Area of Prosthetic Heart Valves. J Heart Valve Dis 2004;13:120-132. Pub Med

4. Scotten LN, Walker DK, Harbott P, de Hart J, Perrault R, Coisne D, et al. The mechanical Bioprosthesis -does valve motion predict thrombogenicity. Abstract #599, Presentation 16th WSCTS, Ottawa, Canada, 17-20 August 2006.

5. Scotten LN, Siegel R. Importance of Shear in Prosthetic Valve Closure Dynamics. J Heart Valve Dis 2011;20:664-672. Link

6. Scotten LN, Siegel R. Thrombogenic potential of transcatheter aortic valve implantation with trivial paravalvular leakage. Ann Transl Med 2014;2(5):43-53. Link

7. Scotten LN, Siegel R. Are anticoagulant independent mechanical valves within reach -fast prototype fabrication and in vitro testing of innovative bi-leaflet valve models. Ann Transl Med 2015;3(14):197-215. Link

8. Chaux A, Richard J. Gray RJ, Stupka JC, Emken MR, Scotten LN, Siegel R. Anticoagulant independent mechanical heart valves: viable now or still a distant holy grail. Ann Transl Med 2016;4(24):525-31. Link

9. Deutsch M-A, Scotten LN, Siegel R, Lange R, Bleiziffer S. Leaflet thrombosis and clinical events after TAVR; Are paravalvular leaks a crucial trigger? EuroIntervention 2018;14:716-717. Link

10. Scotten LN, Blundon D, Deutsch M-A, Siegel R: Violin Plot Data; A concerto of crucial information on valve thrombogenicity classified using laboratory measured valve motion. medRxiv preprint server posts; versions 1-9:2019-2020. Link

11. Lee JH, Rygg AD, Kolahdouz EM, Rossi S, Retta SM, Duraiswamy N, Scotten LN, Craven BA, Griffith BE. Fluid-Structure Interaction models of bioprosthetic heart valve dynamics in an experimental pulse duplicator. Ann Biomed Eng 2020;48(5):1475-1490. Link

12. Lee JH, Scotten LN, Hunt R, Caranasos TG, Vavalle JP, Griffith BE. Bioprosthetic aortic valve diameter and thickness are directly related to leaflet fluttering: Results from a combined experimental and computational modeling study. J Thorac Cardiovasc Surg Open 2021;6:60-81. Link

13. Barrett A, Brown JA, Smith MA, Woodward A, Vavalle JP, Kheradvar A, Griffith BE, Fogelson AL. A model of fluid-structure and biochemical interactions with applications to subclinical leaflet thrombosis. https://arxiv.org/abs/2205.01578v1 Link

14. Carpenter AJ. Commentary: A surgeon's view of engineer's data. JTCVS Open 2021;6:84 Link

15. Obrist D, Carrel TP. Commentary: Leaflet fluttering of bioprosthetic valve –Does it matter? JTCVS Open 2021;6:82-83. Link

16. Chan CHH, Simmonds MJ, Fraser KH, Igarashi K, Ki KK, Murashige T, Joseph MT, Fraser JF, Tansley GD, Watanabe N. Discrete responses of erythrocytes, platelets, and von Willebrand factor to shear. J Biomech 2022: pp1-8. Link

17. Sheriff, J., Wang, P., Zhang, P. Zhang Z., Deng Y, Bluestein D. In Vitro Measurements of Shear-Mediated Platelet Adhesion Kinematics as Analyzed through Machine Learning. Ann Biomed Eng 2021; 49: 3452–3464. Link

18. Cardiovascular implants –cardiac valve prostheses –part 3: heart valve substitutes implanted by transcatheter techniques. *ISO*. 2013;5840-3. Link

19. Tseng E. When valve-in-valve implantation is not sufficient: bioprosthetic Russian dolls. J Thorac Cardiovasc Surg 2016;152(3):624-25. Link

20. Jaiteh LES, Drammeh L, Anderson ST, Mendy J, Ceesay S, D'Alessandro U, Carapetis J, Mirabel M, Erhart A. Rheumatic heart disease in The Gambia: clinical and valvular aspects at presentation and evolution under penicillin prophylaxis. BMC Cardiovasc Disord 2021;21;503-513. Link

21. Zilla P, Brink J, Human P, Bezuidenhout D. Prosthetic heart valves: Catering for the few. Biomaterials 2008;29:385-406. Link

22. Wium E, Jordaan CJ, Botes L , Smit FE. Alternative mechanical heart valves for the developing world. Asian Cardiovasc Thorac Ann 2020;28(7):431-443. Link

23. Wium E. Design, manufacture and hydrodynamic evaluation of a prototype trileaflet mechanical heart valve for aortic valve replacement. MSc Thesis 2020, Stellenbosch University Link

24. Herbertson LH, Deutsch S, Manning KB. Near valve flows and potential blood damage during closure of a bileaflet mechanical heart valve. J Biomech Eng. 2011:133(9):094507-1 to7. Link

25. Soares JS, Sheriff J, Bluestein D. A novel mathematical model of activation and sensitization of platelets subjected to dynamic stress histories. Biomech Model Mechanobiol 2013 Link

26. Ding J, Chen Z, Niu S. Quantification of shear-induced platelet activation: High shear stresses for short exposure time. Artificial Organs 2015;39:576-83. Link

27. Gilchrist IC. Treating hemolysis due to paravalvular leaks: It is all about modifying micro-jets and not the volume of regurgitation. Catheter Cardiovasc Interv 2019;93:720-721. Link

28. Woldendorp K, Indja B, Bannon PG, Fanning JP, Plunkett BT, Grieve SM. Silent brain infarcts and early cognitive outcomes after transcatheter aortic valve implantation: a systematic review and meta-analysis. Eur Heart J 2021; 42:1004-1015. Link

29. Panaich SS, Maor E, Reddy G, Raphael CE, Cabalka A, Hagler DJ, et al. Effect of percutaneous paravalvular leak closure on hemolysis. Catheter Cardiovasc Interv 2019;93:713-719. Link

30. Li W, Gao Z, Jin Z, Qian J. Transient study of flow and cavitation inside a bileaflet mechanical heart valve. Appl Sci 2020; 10:2548; pp1-13. Link

31. Yanagisawa R, Tanaka M, Yashima F, Arai T, Jinzaki M, Shimizu H, et al. Early and late leaflet thrombosis after transcatheter aortic valve replacements a multicenter initiative from the OCEAN-TAVI registry. Circ Cardiovasc Interv 2019;12:e007349. doi: 10.1161/CIRCINTERVENTIONS. 118.007349 Link

32. Carrel T, Dembitsky WP, de Mol B, Obrist D, Dreyfus G, Meuris B, Vennemann BM, Lapeyre D, Schaff H. Non-physiologic closing of bi-leaflet mechanical heart prostheses requires a new tri-leaflet valve design. Int J Cardiol 2020;304:125-127. Link

33. Kolahdouz EM, Bhalla APS, Scotten LN, Craven BA, Griffith BE. A sharp interface Lagrangian-Eulerian method for rigid-body fluid-structure interaction. J. Compu Phys 2021;443 Link

34. Kolahdouz EM, Bhalla APS, Craven BA, Griffith BE. An immersed interface method for discrete surfaces. J. Compu Phys 2020,108854 Link

APPENDIX 1. SUPPLEMENTAL VIDEO

See MPEG 4, animated rotating visualization of prototype BV3D valve structures and full range motion potential.

https://youtu.be/5QmDPbfUvTM U-tube link

APPENDIX 2. SUPPLEMENTAL INFORMATION

A,

Viscoelastic Impedance Adapter (VIA)

Figure 1 includes a schematic of a Windkessel unit comprised of one resistive and two compliance elements. The VIA was characterized a reduced-order model which defines driving and loading conditions for a fluid-structure interaction (FSI) computational modeling method [11-13]. In a saline based test fluid, the reduced-order model elements characterizing the VIA unit are: C_{VIA1} = 0.0010 mL/mm Hg; C_{VIA2} = 0.1456 mL/mm Hg; R_{VIA} = 0.15 mm Hg/mL/s.

B,

Compliance modeling:

The bulk pump source compliances simulated in VIA contain two air volumes C_{VIA1} and C_{VIA2}. These volumes are adjustable and cover physiological range. Air volume settings we used are: C_{VIA1} = 120 ml (0.0010 mL/mm Hg); C_{VIA2} = 50 ml (0.1456 mL/mm Hg); aortic root (C_{root}) and systemic arterial compliance C_{per} = 615 ml. Compliance is defined as the ratio of volume change to pressure difference as follows:

$$\text{Compliance} = \frac{\Delta V}{\Delta P \bullet 1333.2}$$

Where:

ΔV = change in contained air volume in ml

ΔP = pressure difference (mm Hg) caused by volume change ΔV

$\Delta P = P_2 - P_1$

P_1 = initial static pressure in mmHg

P_2 = final static pressure in mmHg

Conversion factor: 1 mmHg = 1333.2 Dynes/cm^2

Air volume$_{max}$ values found experimentally that simulate left ventricle, aortic root, systemic arterial compliance and also calibrated parameters for the reduced-order models with a saline test fluid [11-13] facilitated realistic pressure and flow wave forms under pulsatile flow conditions were:

- R_{VIA} = 0.15 mm Hg/mL/s.
- Aortic root C_{VIA1} = 120 ml = 0.1456 mL/mm Hg
- Output compliance C_{VIA2} = 50 ml
- Aortic root C_{root} = 640 ml= 0.0010 mL/mm Hg
- Left ventricle source compliance air volume C_{VIA2} = 640 ml
- Output compliance air volume = 50 ml
- Peripheral systemic C_{per} = 615 ml

C,
Resistance modeling:
Resistance to flow causes frictional loss of energy and flow container chamber radius is the dominant determinant of resistance. In Figure 1, R_{VIA} and R_{per} offer flow resistance. R_{VIA} consists of a micro-porous water filter section which offers a low fixed resistance to flow (200 c.g.s. units). The peripheral resistance R_{per} offers alterable resistance allowing for operator adjustment of end diastole aortic pressure.

D,
Light source
Phlox® SLLUB Backlight* 50x50mm x 8.5 mm, LED back light source (diffuse red), luminance 5,780 cd/m^2, uniformity 99.24%, wavelength 625±15 nm.
*PHLOX Corp., ZAC de l'Enfant, Aix-en-Provence, France

E, Inter-connection of testing equipment: (next page)

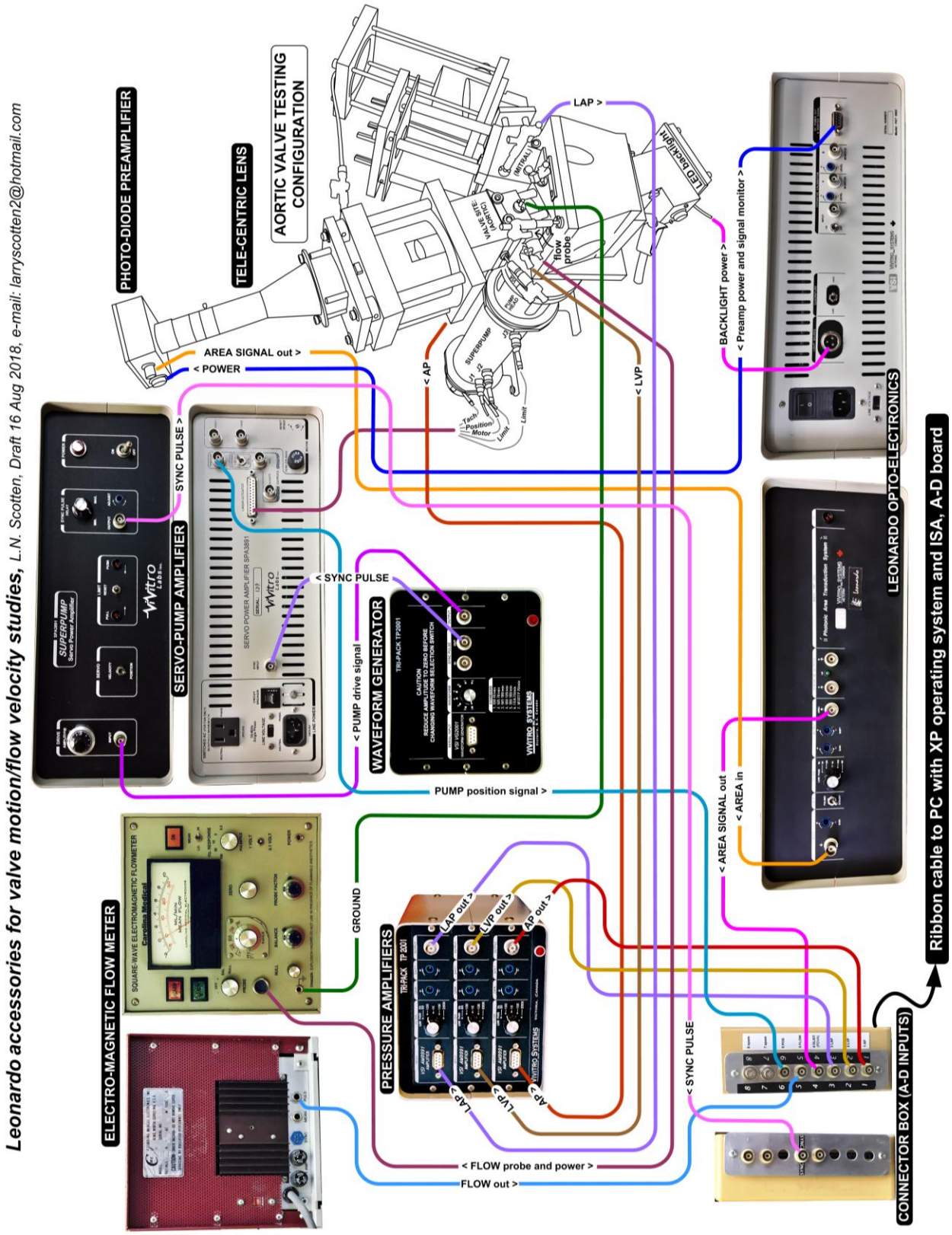

FIGURE 6. Electrical inter-connections for aortic valve testing

***F.** A mining tradition dating back to 1911 used canaries in coal mines to detect carbon monoxide and other toxic gases before they hurt humans. In 1906, Dr. John Scott Haldane proceeded to study asphyxia in coal miners in coal miners and proposed that *"miners carry small animals like mice or canaries to detect levels of gas in their working environment"* This practice was in vogue until 1986. (Sekhar KC, Rao SC. John Scott Haldane: The father of oxygen therapy. Indian J Anaesth 2014;58:350-2.) Link